OPEN ACCESS Freely available online

PLOS ONE

Computational Prediction of Candidate Proteins for S-Nitrosylation in *Arabidopsis thaliana*

Mounira Chaki[1], Izabella Kovacs[1], Manuel Spannagl[2], Christian Lindermayr[1]*

1 Institute of Biochemical Plant Pathology, Helmholtz Zentrum München-German Research Center for Environmental Health, Neuherberg, Germany, **2** Institute of Bioinformatics and Systems Biology, Helmholtz Zentrum München-German Research Center for Environmental Health, Neuherberg, Germany

Abstract

Nitric oxide (NO) is an important signaling molecule that regulates many physiological processes in plants. One of the most important regulatory mechanisms of NO is S-nitrosylation—the covalent attachment of NO to cysteine residues. Although the involvement of cysteine S-nitrosylation in the regulation of protein functions is well established, its substrate specificity remains unknown. Identification of candidates for S-nitrosylation and their target cysteine residues is fundamental for studying the molecular mechanisms and regulatory roles of S-nitrosylation in plants. Several experimental methods that are based on the biotin switch have been developed to identify target proteins for S-nitrosylation. However, these methods have their limits. Thus, computational methods are attracting considerable attention for the identification of modification sites in proteins. Using GPS-SNO version 1.0, a recently developed S-nitrosylation site-prediction program, a set of 16,610 candidate proteins for S-nitrosylation containing 31,900 S-nitrosylation sites was isolated from the entire *Arabidopsis* proteome using the medium threshold. In the compartments ''chloroplast,'' ''CUL4-RING ubiquitin ligase complex,'' and ''membrane'' more than 70% of the proteins were identified as candidates for S-nitrosylation. The high number of identified candidates in the proteome reflects the importance of redox signaling in these compartments. An analysis of the functional distribution of the predicted candidates showed that proteins involved in signaling processes exhibited the highest prediction rate. In a set of 46 proteins, where 53 putative S-nitrosylation sites were already experimentally determined, the GPS-SNO program predicted 60 S-nitrosylation sites, but only 11 overlap with the results of the experimental approach. In general, a computer-assisted method for the prediction of targets for S-nitrosylation is a very good tool; however, further development, such as including the three dimensional structure of proteins in such analyses, would improve the identification of S-nitrosylation sites.

Citation: Chaki M, Kovacs I, Spannagl M, Lindermayr C (2014) Computational Prediction of Candidate Proteins for S-Nitrosylation in *Arabidopsis thaliana*. PLoS ONE 9(10): e110232. doi:10.1371/journal.pone.0110232

Editor: Yu Xue, Huazhong University of Science and Technology, China

Received April 11, 2014; **Accepted** September 17, 2014; **Published** October 21, 2014

Data Availability: The authors confirm that all data underlying the findings are fully available without restriction. All relevant data are within the paper and its Supporting Information files.

Funding: This work was supported by Marie Curie Intra-European Fellowship within the 7th European Community Framework Programme (Call: FP7-PEOPLE-2011-IEF) under grant agreement n°300176 and the Bundesministerium für Forschung und Bildung. The funders had no role in study design, data collection and analysis, decision to publish, or preparation of the manuscript.

Competing Interests: The authors have declared that no competing interests exist.

* Email: lindermayr@helmholtz-muenchen.de

Introduction

NO is a membrane-permeable free radical that plays a central role in a broad spectrum of physiological processes in plants, including germination, flowering, root development, hormonal signaling, senescence, and the establishment of adaptive responses against biotic and abiotic stress [1–9]. NO and related nitrogen species that are considered reactive can mediate various post-translational modifications (PTMs), such as metal nitrosylation, tyrosine nitration, and cysteine S-nitrosylation. Cysteine S-nitrosylation is the term used to describe the covalent binding of an NO group to a protein cysteine (Cys) residue. This PTM is considered one of the most important molecular mechanisms by which NO regulates protein functions and cell signaling and has been shown to alter protein activities, protein-protein interactions, and subcellular localization under both normal and pathological conditions [10–13].

A number of indirect MS-based proteomics approaches have been developed for the identification of S-nitrosylated proteins and their modification sites from complex biological samples [14,15]. The biotin switch technique (BST) is the most widely used method and is based on the conversion of S-nitrosylated Cys to biotinylated Cys. Such labeling allows the detection of S-nitrosylated proteins using specific anti-biotin antibodies and their isolation by affinity chromatography using neutravidin matrices. The proteins can then be identified using mass spectrometry. S-nitrosoglutathione (GSNO) is the most abundant low-molecular-weight S-nitrosothiol in plant cells and is a physiological NO reservoir and NO donor. This molecule can transfer its NO moiety to protein cysteine residues via trans-nitrosylation. GSNO has often been used to generate S-nitrosylated proteins in extracts for the subsequent isolation and identification of S-nitrosylated proteins [16–20].

The identification of redox-sensitive cysteine residues is important for understanding the regulatory functions of NO. Cysteine residues exhibiting a low-pKa sulfhydryl group are particularly susceptible to certain types of redox modification [21]. Several research groups have attempted to define consensus motifs

for S-nitrosylation by comparing the amino acid sequences around identified target cysteine residues. Such analyses have revealed that the target cysteine residues often lie within an acid-base or hydrophobic motif [22]. In contrast, other studies have revealed that the primary sequence of the surrounding amino acid residues has no significant effect on the reactivity of cysteines towards S-nitrosylation at the peptide level [23]. Greco et al. (2006) supported the idea of extending the motif beyond the primary sequence to include hydrophobic motifs surrounding the identified cysteine residues [24]. Recently, 70 known S-nitrosylated sites were used to identify general structures associated with S-nitrosylation. The results obtained revealed that proximal acid–base motif, Cys pKa, sulfur atom exposure, and Cys conservation or hydrophobicity in the vicinity of the modified cysteine do not predict S-nitrosylation specificity. Instead, this analysis identified a revised acid-base motif that is located farther from the cysteine and in which the charged groups are exposed [25].

Many studies have been performed to identify and characterize S-nitrosylated proteins in plants [26]. The pioneer analysis of S-nitrosylated proteins was conducted in 2005 [16]. In this work, 63 proteins from GSNO-treated *Arabidopsis* cell culture extracts and 52 proteins from NO-treated leaves were identified as possible NO targets. In addition, Romero-Puertas and colleagues found 16 *Arabidopsis* proteins that were differentially S-nitrosylated under hypersensitive responses [27]. Moreover, endogenous S-nitrosylated proteins have been identified in an *Arabidopsis* cell culture under salt stress [28]. To date, more than two hundred proteins have been identified as putative targets for S-nitrosylation in *Arabidopsis* using proteomics approaches based on the biotin switch assay or related techniques, however only in the minority of them the exact S-nitrosylation sites have been identified. Moreover, such analyses have also been performed in other plant species such as in citrus plants exposed to salinity [29], a rice mutant overproducing NO [30], pea-leaf peroxisomes under abiotic stress [31], and a tobacco cell suspension treated with cryptogein [32]. The S-nitrosylated proteins identified from plant proteome studies have been shown to participate in major cellular activities, notably primary and secondary metabolism, protein folding and genetic information processing, photosynthesis, cellular architecture, and responses to biotic and abiotic stresses [33]. Although the number of plant proteins that have been identified as putative targets for S-nitrosylation has drastically increased during recent years, studies identifying the NO-sensitive cysteine residues involved remain rare. These analyses are essential for a better understanding of the function of protein S-nitrosylation in plants [33].

In contrast to the technical difficulties associated with experimental methods, the computational analysis of PTMs is an attractive alternative. The use of computational predictors can identify a number of potential candidates and rapidly generate useful information. Currently, approximately 170 databases and computational tools have been developed for PTM analysis [34]. The algorithms used in this field include iGPS 1.0, which is used to predict phosphorylation [35], CSS-Palm 4.0, which is used to predict S-palmitoylation [36], GPS-SUMO 1.0, which is used to predict sumoylation [37], and GPS-YNO2, which is used to predict protein nitration [38]. Moreover, several programs and algorithms have been developed to predict cysteine residues that are susceptible to S-nitrosylation, including SNOSite, iSNO-PseAAC, iSNO-AAPair, and GPS-SNO 1.0 [39–42].

In this study, we used GPS-SNO 1.0 to identify candidate proteins for S-nitrosylation within the *Arabidopsis* proteome (27,416 proteins). In total, 31,907 S-nitrosylated sites were predicted in 16,610 (approximately 61%) candidate proteins using the medium threshold. Potential target proteins were detected in all cellular compartments and ranged from 37% to 86% of the total number of proteins per compartment. More than 70% of the S-nitrosylated candidates identified were in the "chloroplast", "CUL4-RING ubiquitin ligase complex", and "membrane" compartments. In most compartments, the proportion of S-nitrosylation candidates was approximately 60%. Moreover, the 10% of S-nitrosylation sites with the highest prediction confidence were extracted for further study. This group comprised 3,190 sites in 3,005 target proteins. These candidates were detected in all compartments and ranged from 5% to 17% of the total number of proteins per compartment. These targets were enriched in the "chloroplast" (17%), "intracellular" (15%), and "plasmodesmata" (14%) compartments. In most compartments, the percentage of proteins predicted as S-nitrosylation candidates was approximately 10%. The high proportion of proteins identified as S-nitrosylation candidates reflects the importance of redox signaling in these compartments. An analysis of the functional distribution of the predicted candidates showed that the group with the highest prediction rate was the process "signaling". Moreover, a set of 46 *Arabidopsis* proteins, where 53 putative S-nitrosylation sites were previously determined using a BST-based approach, was analysed with the GPS-SNO program. The computational method predicted 60 S-nitrosylation sites within these proteins, but only 11 overlap with the results of the BST-based approach. In general, the currently available algorithm appears to be a useful tool for characterizing the S-nitrosylome but requires further improvement regarding its accuracy in identifying S-nitrosylation sites.

Materials and Methods

Data collection

First, 27,416 amino acid sequences were downloaded from the most recent version of the *Arabidopsis* information resource TAIR (TAIR10, www.arabidopsis.org). For all subsequent analyses, only one representative gene model was used per locus.

Comparison of prediction performance

To evaluate and compare the prediction performance of four S-nitrosylation prediction programs, we calculated 3 parameters (accuracy, sensitivity, and specificity) according to the definitions described previously [42]. The 4 prediction programs tested were GPS-SNO 1.0 (using the medium threshold condition), iSNO-PseAAC, iSNO-AAPair, and SNOSite [39-41].

Prediction of SNO sites using GPS-SNO software

Group-based Prediction System (GPS-SNO 1.0) software was used to predict S-nitrosylation sites [42]; this program can be executed online or downloaded at http://sno.biocuckoo.org/. In all analyses, 27,416 *Arabidopsis* amino acid sequences in FASTA format were submitted for use in predicting S-nitrosylation sites under the medium threshold condition using the batch prediction tool of the GPS-SNO 1.0 software. The predicted S-nitrosylation sites were extracted into an Excel file for further analysis.

Subcellular compartmentalization of *Arabidopsis* proteins

To determine the cellular localization of all gene predictions in *Arabidopsis*, we utilized gene ontology terms (GO) obtained from the TAIR10 annotation release (ftp://ftp.arabidopsis.org/home/tair/Ontologies/Gene_Ontology/) and filtered these terms for terms categorized as "cellular component". The distribution of proteins among the individual localization categories was plotted for all categories comprising more than 100 assignments.

MapMan analysis of the predicted candidate proteins

Protein functional classification was performed according to the MapMan Ontology of *Arabidopsis* proteins, version 3.5.1R2 (http://mapman.gabipd.org/web/guest/mapman).

Results and Discussion

In recent years, many experimental methods have been developed for the identification of S-nitrosylated proteins and the mapping of SNO-sites. The BST and related methods have enabled the high-throughput identification of hundreds of novel targets for S-nitrosylation [16,18,43-45]. However, these methods have several limitations, especially regarding the detection of low-abundance or unstable proteins or of proteins that are present only in specific tissues/organs that are difficult to handle, e.g., meristems or epidermis. Therefore, more sensitive approaches are required. ProteoMiner is a technology allowing the enrichment of low-abundance proteins [46]. However, the extracted proteins are denatured by the harsh conditions required for protein elution. Therefore, this method cannot be used in combination with the BST until a method for enriching low-abundance proteins under native conditions is established. Computational methods can overcome such technical difficulties because the analyses can be performed using the complete protein datasets that are available in databases. Thus, a nearly complete map of candidates for S-nitrosylation can be generated, providing a good starting point for more detailed, experimental approaches.

1. A comparison of programs used to predict S-nitrosylation sites

Previously, we compared three programs that are used to predict S-nitrosylation sites in proteins [26]. Here, we extended this study by including a fourth program and including all plant proteins in which modified cysteine residues have been verified using mass spectrometry and for which the physiological functions are known (Table 1). The programs GPS-SNO 1.0, iSNO-PseAAC, iSNO-AAPair, and SNOSite were tested. The performances of the 4 programs in predicting S-nitrosylation were evaluated (Table S1) as previously defined [42], using the 12 characterized S-nitrosylated proteins listed in Table 1. GPS-SNO performed best according to the three criteria chosen (accuracy, sensitivity, and specificity; 82.2%, 50%, and 87.9%, respectively, Table S1). The SNOSite software predicted almost all cysteine residues present as targets for S-nitrosylation, with accuracy and specificity of 25% and 13%, respectively, which implies that S-nitrosylation is very unspecific. The programs iSNO-PseAAC and iSNO-AAPair presented higher accuracy and specificity than SNOSite (Table S1), but their correlation with actual sites remained low. Significantly better predictions appeared possible when using the GPS-SNO 1.0 software, which exhibited a much lower rate of false positives. Approximately 60% of the proteins that were found to be S-nitrosylated using mass spectrometry were predicted using the GPS-SNO 1.0 software (which was developed by Xue and colleagues [42]). The authors of this program have improved their previous algorithm, GPS 2.0 (Group-based Prediction System), which was used for the prediction of kinase-specific phosphorylation sites, and have released GPS 3.0 [47]. Based on this algorithm, they developed the computational software GPS-SNO 1.0 for the prediction of S-nitrosylation sites. The performance of the GPS 3.0 algorithm at predicting S-nitrosylation was much better than that obtained using several other approaches, providing an accuracy of 75.70%, a sensitivity of 53.32% and a specificity of 80.11% under the low threshold condition. GPS-SNO 1.0 was applied to a test set of 485 potentially S-nitrosylated proteins collected from PubMed. These proteins were identified in large- or small-scale studies, and the actual S-nitrosylation sites have not been experimentally determined. Of the analyzed proteins, 371 (approximately 76%) were predicted to be S-nitrosylated at one or more potential S-nitrosylation sites.

2. Prediction of S-nitrosylation candidate proteins using the GPS-SNO 1.0 program

For the computer-based prediction of the S-nitrosylation of *Arabidopsis* target proteins, 27,416 amino acid sequences were extracted from the TAIR 10 database (www.arabidopsis.org) (Table S2). Of these proteins, 25,785 (94%) contain at least one cysteine residue; in total, 207,473 cysteine residues were found. All of the *Arabidopsis* amino acid sequences were analyzed with GPS-SNO 1.0 using the medium threshold, as recommended by Xue and colleagues [42]. In total, 31,907 (approximately 15% of all Cys residues) S-nitrosylation sites were predicted in 16,610 proteins (60%) (Table 2 and Table S2 and S3), suggesting that redox-related processes are closely regulated by a small number of redox-sensitive cysteine residues. The high number of putative candidate proteins reflects the importance of redox-signaling in general. Redox homeostasis during development is an evolutionary conserved strategy and the common origin of redox sensing indicate that organisms evolved similar strategies for utilizing redox-signaling during development [48]. In plant with impaired NO/S-nitrosothiol (SNO) homeostasis the importance of balancing NO/SNO levels for plant growth and development become apparent. For instance, S-nitrosoglutathione reductase knock-out plants have higher SNO levels in comparison to wild type plants and display a lot of different developmental defects, such as delayed seed germination, reduced growth, reduced trichome density, increased number of branched shoots, and generation of more flowers, which are smaller and develop to smaller siliques containing smaller seeds [49]. Moreover, leaf shape, 2,4-D sensitivity, and hypocotyl elongation is affected [50]. But S-nitrosylation of proteins might have not only a signaling function. A protection of cysteine residues against irreversible oxidation is also described [51,52]. In this way proteins can be protected against oxidative damage and after reduction they can fulfil their physiological function again.

On the other side, the high number of putative candidate proteins might indicate a high rate of false-positive predictions. Therefore, we extracted the 10% of predicted sites with the highest prediction confidence by ranking the prediction results according to the raw score divided by the threshold (Cutoff) for a particular cluster. These sites (3,190) were localized to 3005 different proteins, which comprise 18% of all predicted S-nitrosylation candidates (Table 2 and Table S2 and S3). Similarly, computational prediction has also been used for other post-translational modifications of target proteins. In the *Arabidopsis* proteome, the phosphorylation hotspot prediction algorithm has predicted 13,677 P-hotspots in 9,599 proteins corresponding to 7,847 unique genes [53]. The cited study provides a new bioinformatic method to identify phosphorylation hotspots and provides the basis for further investigation of novel candidate P-hotspots. Moreover, in the human proteome, nitration-sensitive tyrosine residues have been predicted using GPS-YNO2, a recently described 3-nitrotyrosine prediction algorithm [54]. In total, 9.27% (27,977) of all tyrosine residues (301,091) were predicted to be nitration targets. Collectively, these studies demonstrate the feasibility of using predicted datasets for whole-proteome analyses.

Table 1. Computational prediction of *S*-nitrosylation sites from experimentally identified *S*-nitrosylated proteins in plants using GPS-SNO 1.0, iSNO-PseAAC, iSNO-AAPair, and SNOSite software.

Protein name	Accession number	Total number of Cys	Physiological function demonstrated	Cys-NO sites identified by LC-MS/MS	Cys-NO sites predicted by GPS-SNO 1.0	Cys-NO sites predicted by iSNO-PseAAC	Cys-NO sites predicted by iSNO-AAPair	Cys-NO sites predicted by SNOSite	Reference
Methionine adenosyltransferase 1	At1g02500	8	Inhibited	C_{114}	C_{114}	C_{161}	C_{31}, C_{90}, C_{161}	C_{20}, C_{31}, C_{42}, C_{73}, C_{90}, C_{114}, C_{161}	[85]
Metacaspase 9	At5g04200	7	Inhibited	C_{147}	C_{17}, C_{147}	C_{17}, C_{29}	C_{117}	C_{17}, C_{29}, C_{117}, C_{147}, C_{309}	[81]
Peroxiredoxin II E	At3g52960	2	Inhibited	C_{121}	C_{121}	C_{121}, C_{146}	C_{121}	C_{121}, C_{146}	[86]
NPR1	At1g64280	17	Inhibited	C_{156}	C_{156}, C_{385}	C_{212}, C_{306}	C_{223}, C_{306}, C_{394},C_{457}	C_{82}, C_{150}, C_{155}, C_{156}, C_{160}, C_{212}, C_{223}, C_{297}, C_{306}, C_{378}, C_{385}, C_{394}, C_{457}, C_{511}, C_{529}	[83]
GAPDH	At1g13440	2	Inhibited	C_{156}, C_{160}	C_{156}, C_{160}	_	_	C_{156}, C_{160}	[87]
SABP3	At3g01500	7	Inhibited	C_{280}	C_{34}, C_{173}, C_{280}	C_{230}, C_{257}	C_{34}	C_{34}, C_{167}, C_{173}, C_{230}, C_{257}, C_{277}, C_{280}	[88]
Transcription factor-TGA1	At5g65210	4	Activated	C_{172}, C_{287}	C_{172}	_	_	C_{172}, C_{260}, C_{266}, C_{287}	[19]
NADPH oxidase	At5g47910	10	Inhibited	C_{890}	_	C_{208}, C_{387}, C_{433}, C_{480}, C_{695}	C_{412}, C_{480}, C_{695}, C_{890}	C_{208}, C_{410}, C_{412}, C_{433}, C_{480}, C_{651}, C_{695}, C_{825}, C_{890}	[89]
cALD2	At2g36460	6	Inhibited	C_{173}	C_{68}, C_{326}	C_{326}	C_{208}	C_{68}, C_{173}, C_{197}, C_{208}, C_{326}	[90]
TIR1	At3g62980	23	Activated	C_{140}	C_{516}, C_{551}	C_{34}, C_{53}, C_{121}, C_{140}, C_{155}, C_{210}, C_{269}, C_{288}, C_{311}, C_{405}, C_{480}, C_{491}	C_{121}, C_{140}, C_{405}, C_{551}	C_{34}, C_{44}, C_{53}, C_{121}, C_{140}, C_{155}, C_{193}, C_{210}, C_{264}, C_{269}, C_{288}, C_{311}, C_{337}, C_{371}, C_{405}, C_{480}, C_{491}, C_{516}, C_{523}, C_{551}	[91]
CDC48	Q1G0Z1	14	Inhibited	C_{110}, C_{526}, C_{664}	C_{426}, C_{576}	C_{74}, C_{82}, C_{110}, C_{526}, C_{539}, C_{576}, C_{664}, C_{699}	C_{74}, C_{426}, C_{539}, C_{576}	C_{74}, C_{82}, C_{110}, C_{179}, C_{189}, C_{272}, C_{419}, C_{426}, C_{539}, C_{576}, C_{664}, C_{695}, C_{699}	[32]
AtMYB30	At3g28910	7	Inhibited	C_{53}	C_{6}	C_{6}, C_{7}, C_{49}, C_{53}, C_{257}, C_{289}	C_{6}, C_{7}	C_{49}, C_{53}, C_{257}, C_{289}, C_{290}	[92]

Amino acid sequences were downloaded from the most recent version of the *Arabidopsis* information resource TAIR (TAIR10, www.arabidopsis.org) and subjected to the different programs for prediction of S-nitrosylation sites. NPR1, non-expresser of pathogenesis related genes 1; GAPDH, glyceraldehyde 3-phosphate dehydrogenase; SABP3, salicylic acid binding protein 3; TGA1, TGACG motif binding factor; cALD2, cytosolic fructose 1,6-bisphosphate aldolase; TIR1, transport inhibitor response 1; CDC48, cell division cycle 48; AtMYB30, *Arabidopsis thaliana* MYB transcription factor.

C in bold, matched cysteine residues, "_" not predicted

doi:10.1371/journal.pone.0110232.t001

Table 2. Prediction of *Arabidopsis* candidate proteins for S-nitrosylation using the GPS-SNO 1.0 software.

	Arabidopsis proteome	Candidate proteins for *S*-nitrosylation	The highest 10% high-confident predicted candidates
Total number of proteins	27,416	16,610 (60%)	3,005 (18%)
Total number of Cys-NO	207,473	31,907 (15%)	3,190 (10%)

Arabidopsis amino acid sequences were extracted from TAIR 10 database (www.arabidopsis.org) and analysed by GPS-SNO 1.0 software using medium threshold condition. The 10% of predicted sites with the highest prediction confidence were determined by ranking the prediction results according to the raw score divided by the threshold (Cutoff) for a particular cluster.

doi:10.1371/journal.pone.0110232.t002

3. Subcellular compartment classification of *Arabidopsis* proteins

To determine whether the identified candidates for S-nitrosylation are enriched in distinct subcellular compartments (Text S1), all *Arabidopsis* proteins and the predicted candidates were assigned to subcellular locations according to gene ontology (GO) terms using cellular component classifications (Table S4). In Table 3, only compartments with more than 100 representatives are listed. An analysis of the subcellular localization of all *Arabidopsis* proteins revealed that most were assigned to the "nucleus" (9,214 proteins) or to "membranes" (4,389 proteins). The predicted S-nitrosylation candidate proteins were also located in other compartments, comprising 37% to 86% of the total protein content in each compartment (Table 3). Similar results have been found experimentally in *Arabidopsis* suspension cell cultures: S-nitrosylated proteins were found in almost all cell

Table 3. Subcellular compartment classification of *Arabidopsis* proteins.

Compartments	Total number of proteins	Candidate proteins for *S*-nitrosylation	Candidate proteins for *S*-nitrosylation harboring the highest 10% high-confident predicted sites
Chloroplast	3795	3259 (86%)	659 (17%)
CUL4-RING ubiquitin ligase complex	121	91 (75%)	13 (11%)
Membrane	4389	3257 (74%)	493 (11%)
Plasmodesmata	848	596 (70%)	116 (14%)
Vacuole	799	556 (70%)	79 (10%)
Cell wall	469	314 (67%)	45 (10%)
Plant-type cell wall	264	176 (67%)	26 (10%)
Endosome	232	153 (66%)	13 (6%)
Trans-Golgi network	219	144 (66%)	13 (6%)
Cytoplasm	3461	2222 (64%)	364 (11%)
Nucleus	9214	5924 (64%)	1118 (12%)
Extracellular region	2390	1512 (63%)	232 (10%)
Intracellular	1015	630 (62%)	148 (15%)
Cytosol	1468	903 (62%)	151 (10%)
Integral to membrane	808	503 (62%)	67 (8%)
Golgi apparatus	877	539 (61%)	65 (7%)
Plastid	289	172 (60%)	37 (13%)
Peroxisome	170	99 (58%)	17 (10%)
Mitochondrion	3048	1744 (57%)	323 (11%)
Cytosolic ribosome	304	164 (54%)	30 (10%)
Apoplast	390	208 (53%)	35 (9%)
Endoplasmic reticulum	517	270 (52%)	26 (5%)
Anchored to membrane	237	120 (51%)	16 (7%)
Ribosome	384	143 (37%)	33 (9%)
Cellular component	1917	705 (37%)	149 (8%)

Total number of proteins, number of predicted candidates for *S*-nitrosylation, and the number of candidates with the highest 10% prediction confidence were assigned to their subcellular localization according to gene ontology cellular component classification. The prediction confidence was calculated by dividing the raw score value by the cutoff value of a particular cluster.

doi:10.1371/journal.pone.0110232.t003

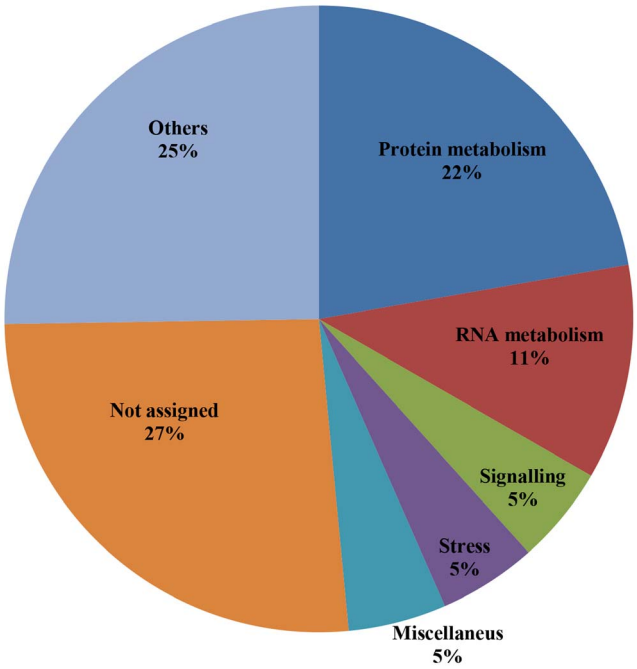

Figure 1. Functional distribution of predicted candidate proteins for *S*-nitrosylation has been determined using the MapMan Ontology tool (http://mapman.gabipd.org/). Others; include all functional classes which have less than 5% of predicted candidates.
doi:10.1371/journal.pone.0110232.g001

compartments [28]. Moreover, a similar distribution was also observed in animal cells [55]. Interestingly, the predicted candidates are most enriched in the "chloroplast", "CUL4-RING ubiquitin ligase complex", and "membrane" compartments (86%, 75%, and 74%, respectively), suggesting that redox-related processes play important roles in these locations.

The nucleus is an important sub-cellular organelle that contains almost all of the genetic information required for the regulation of cellular processes. Interestingly, a high number of S-nitrosylation candidates was predicted for the "nucleus" compartment (5,924 proteins, 64% of the total), which also contained a high proportion of the proteins that harbored the 10% of sites that were predicted with the highest confidence (1,118 proteins, 12% of the total).

The 10% of S-nitrosylation sites that were predicted with the highest confidence were also found in all compartments at levels of 5% to 17% (Table 3). In particular, the compartments "chloroplast" (17%), "intracellular" (15%), and "plasmodesmata" (14%) appeared to be enriched in the sites predicted with high confidence. Interestingly, chloroplast proteins exhibited the highest percentage of S-nitrosylation candidates in both analyses. Chloroplasts are sources of redox intermediates and chloroplast signaling pathways are triggered by the redox state of the plastochinone pool, the thioredoxin system, and the acceptor availability at photosystem I [56]. Moreover, discrete redox signaling pathways regulate photosynthetic light-harvesting and chloroplast gene transcription [57]. Production of NO in plant cells arise from several different pathways and in different organelles, including chloroplasts [58,59] and target sites of NO in chloroplasts have been found in photosystem I and II, in the cytochrome *b6f* complex and in carbon dioxide reduction processes [60]. Although the chloroplast S-nitrosylome has not been analyzed yet, alterations in ribulose-1,5-bisphosphate carboxylase/oxygenase S-nitrosylation inactivated its carboxylase activity in *Brassica juncea* [61]. Furthermore, chloroplastic triosephosphate isomerase (TPI) was already identified as target for S-nitrosylation in rice, citrus, and *Chlamydomonas reinhardtii*, suggesting that this type of modification might be involved in the regulation of chloroplastic TPI activity [29,30,62,63]. Moreover, chloroplasts have been discussed as a source and a target of cellular redox regulation [56] and therefore might represent a favorable microenvironment for S-nitrosylation in *Arabidopsis*.

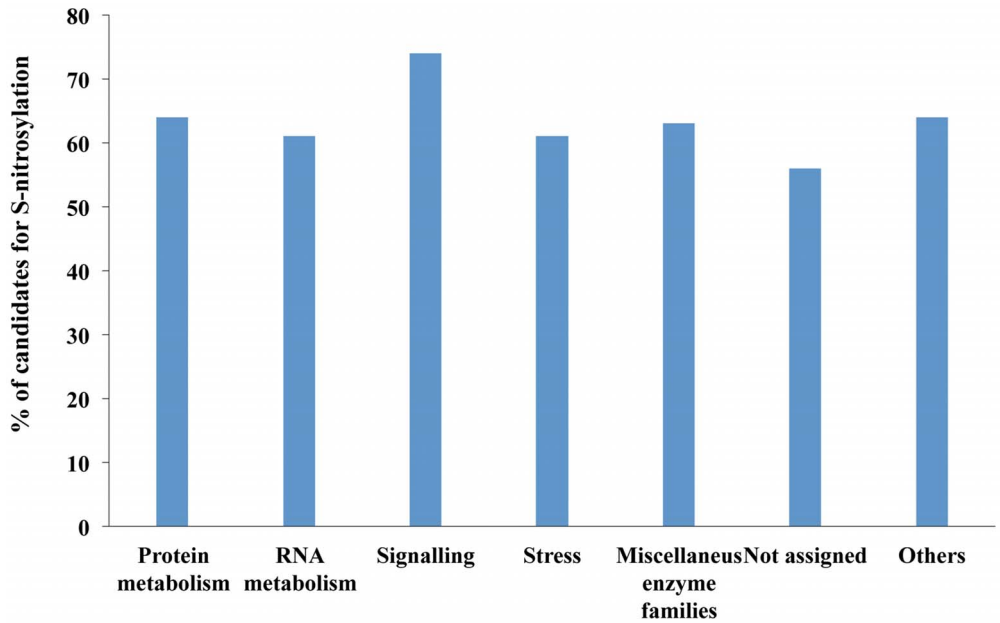

Figure 2. Percentage of candidate proteins for *S*-nitrosylation in different functional categories. Functional assignment has been done using the MapMan Ontology tool (http://mapman.gabipd.org/web/guest/mapman).
doi:10.1371/journal.pone.0110232.g002

Table 4. Percentage of predicted candidate proteins for *S*-nitrosylation in signaling subclasses.

Signaling subclasses	Total proteins	Candidate proteins for *S*-nitrosylation
14-3-3 proteins	15	15 (100%)
Light	117	98 (84%)
Lipids	6	5 (83%)
MAP kinases	50	40 (80%)
Receptor kinases	1067	843 (79%)
Phosphinositides	98	76 (78%)
Sugar and nutrient physiology	82	58 (71%)
G-proteins	243	157 (65%)
Unspecified	8	5 (62%)
Calcium	230	141 (61%)
Miscellaneus enzyme families	41	21 (51%)
Phosphorelay	5	1 (20%)

Functional classification of the predicted candidates has been done using the MapMan Ontology software (http://mapman.gabipd.org/web/guest/mapman).
doi:10.1371/journal.pone.0110232.t004

In most compartments, the percentage of proteins predicted as S-nitrosylation candidates using the medium threshold ranged from 51% to 70%. The smallest proportion of S-nitrosylation candidates was located in the ''ribosome'' compartment (37%). Ribosomes comprise the basic machinery that decodes genetic information into proteins. Increasing numbers of studies on ribosome biogenesis have been performed on *Arabidopsis*. Ribosomal protein functions have been demonstrated in embryo biogenesis, leaf and flower development, vacuolar trafficking, and the UV response [64–70]. However, the lowest percentages of predicted targets among the 10% of sites predicted with the highest confidence were found in the ''endoplasmic reticulum'' (5%), ''trans-Golgi network'' (6%), and ''endosome'' (6%) compartments. Several previous studies have demonstrated that S-nitrosylated proteins were localized in various organelles, including the cell membrane [71], mitochondria [72,73], the nucleus [74], the endoplasmic reticulum, the Golgi and cytosol [75], the peroxisome [31], and the apoplast [76]. This suggests that protein S-nitrosylation can occur in all subcellular compartments [77].

4. Functional distribution of *Arabidopsis* S-nitrosylation candidate proteins

To analyze the functional classification of the predicted candidates, 16,610 predicted proteins were subjected to analysis using the MapMan Ontology of *Arabidopsis* proteins (http://mapman.gabipd.org/web/guest/mapman). Most of the candidates belong to unknown categories (not assigned) or others, including categories containing less than 5% of candidates (Figure 1). Most of the candidates assigned to known categories are involved in protein and RNA metabolism (22% and 11% of all candidates, respectively), signaling (5%) and stress-related processes (5%). The proportion of predicted candidates in known functional categories was calculated in relation to the total number of proteins of each category; the results showed that approximately 60% of the proteins in each category were S-nitrosylation candidates (Figure 2). The signaling category presented the highest proportion of S-nitrosylation candidates (70%). A more detailed analysis of this group revealed that 70% to 100% of the subclasses ''14-3-3 family proteins'', ''light'', ''lipids'', ''MAP and receptor kinases'', ''phosphoinositides'', and ''sugar and nutrient physiology'', are S-nitrosylation candidates (Table 4). 14-3-3 proteins have previously been identified as S-nitrosylation targets in *Arabidopsis* [16,28] and in mesangial cells [78]. 14-3-3 proteins represent an emerging family of proteins and protein domains that bind to serine/threonine-phosphorylated residues. These proteins regulate key proteins that are involved in several physiological processes, including intracellular signaling, apoptosis, cell cycling, and transcriptional regulation. 14-3-3 proteins also act as adaptor molecules that stimulate protein-protein interactions and regulate the subcellular localization of proteins [79]. Interestingly, the 10% of sites predicted with the highest confidence in the large-scale prediction study showed the same functional classification pattern as that for all S-nitrosylated proteins (Figure S1). The functional distribution of the predicted S-nitrosylation candidates is similar to that of the major classes of S-nitrosylated proteins that have been identified experimentally in *Arabidopsis* [16,27,28,80].

5. A comparison of experimentally identified candidates with the candidates predicted using GPS-SNO 1.0 software

Two-hundred sixty-three proteins have previously been identified experimentally in *Arabidopsis thaliana* as S-nitrosylation candidates based on the BST [16,18,19,27,28,80–83]. These proteins were detected using large- and small-scale studies, most of which did not determine the exact S-nitrosylation sites experimentally. To compare the results of the computational predictions with experimental data, we analyzed these datasets using GPS-SNO. Interestingly, 160 proteins (approximately 61%) that were identified using the biotin switch approach were also predicted by the GPS-SNO software (using the medium threshold) as S-nitrosylation candidates.

In a more detailed analysis, Fares et al. experimentally identified 53 S-nitrosylation sites on 46 proteins in an *Arabidopsis* cell suspension using BS-ICAT technology [28]. However, these identified S-nitrosylation sites were not further verified on the biochemical and physiological level meaning that these S-nitrosylation sites/proteins are still candidates. This set of proteins was also analyzed using the GPS-SNO 1.0 software under the medium threshold condition (Table 5). This analysis revealed that approximately 74% of proteins (34 proteins) that were identified as S-nitrosylated using BS-ICAT were also predicted as S-nitrosylation candidates using GPS-SNO. To compare the candidate

Table 5. Prediction of *S*-nitrosylated sites from experimentally identified *S*-nitrosylated proteins by GPS-SNO software.

Accession number	Cys-NO site identified by BS-ICAT	Cys-NO site predicted by GPS-SNO	NO-peptide sequence predicted by GPS-SNO
AT1G04710	C_{130}	C_{184}	KFEQAHNCLLPMGIT
AT1G04710	-	C_{363}	FASQFVYCRNKLGLD
AT1G04710	-	C_{394}	LGATGARCVATLLHE
AT1G04710	-	C_{417}	RFGVVSMCIGSGMGA
AT1G07890	C_{32}	C_{19}	YKKAVEKCRRKLRGL
AT1G07930	C_{87}	C_{111}	TGTSQADCAVLIIDS
AT1G09780	C_{100}	C_{355}	NGVSTFACSETVKFG
AT1G19570	C_{20}	C_{6}	**MALEICVKAAVGA
AT1G22300	C_{98}	$\mathbf{C}_{98}$	EDELAKVCNDILSVI
AT1G35720	C_{111}	$\mathbf{C}_{111}$	QVLMEVACTRTSTQL
AT1G47128	C_{233}	C_{161}	DQGGCGSCWAFSTIG
AT1G47128	C_{342}	$\mathbf{C}_{342}$	IASSSGKCGIAIEPS
AT1G47128	-	C_{200}	DTSYNEGCNGGLMDY
AT1G56070	C_{370}	C_{131}	GALVVVDCIEGVCVQ
AT1G56070	-	C_{448}	ETVEDVPCGNTVAMV
AT1G60710	C_{198}	C_{5}	***MAEACGVRRMKL
AT1G60710	-	C_{254}	KIVYEKVCAISEKKG
AT1G63000	C_{162}	-	-
AT1G65930	C_{75}	C_{297}	LMTSVLVCPDGKTIE
AT1G65930	C_{363}	$\mathbf{C}_{363}$	TEKLEAACVGTVESG
AT1G65930	C_{269}	-	-
AT1G73010	C_{98}	C_{165}	GTCPPNMCKGLIIER
AT1G77120	C_{243}	C_{10}	TTGQIIRCKAAVAWE
AT1G77120	-	C_{271}	GVDRSVECTGSVQAM
AT1G78830	C_{374}	-	-
AT2G31390	C_{298}	-	-
AT2G39730	C_{175}	C_{451}	NLPVPEGCTDPVAEN
AT2G44350	C_{108}	C_{210}	WEPTYEDCLNLIARV
AT2G45290	C_{440}	$\mathbf{C}_{440}$	TRNLSQQCLNALAKA
AT2G45290	-	C_{245}	EGISNEVCSLAGHWG
AT3G08580	C_{130}	$\mathbf{C}_{130}$	PYKGIGDCFGRTIKD
AT3G09820	C_{323}	-	-
AT3G09840	C_{109}	C_{425}	CTEAALQCIREKMDV
AT3G09840	-	C_{575}	KARQSAPCVLFFDEL
AT3G11940	C_{175}	C_{69}	KRFRKAQCPIVERLT
AT3G17240	C_{372}	-	-
AT3G47370	C_{39}	-	-
AT3G51800	C_{178}	-	-
AT3G53870	C_{134}	C_{97}	KVNNRGLCAIAQAES
AT3G55440	C_{218}	C_{13}	FVGGNWKCNGTAEEV
AT3G55440	C_{127}	$\mathbf{C}_{127}$	QGLKVIACVGETLEE
AT3G56310	C_{311}	C_{117}	IHVNIDDCWSNLLRD
AT3G56310	-	C_{422}	AQVDAHDCHMYVLTP
AT3G61440	C_{72}	C_{16}	LRRETIPCFSHTVRK
AT3G61440	-	C_{87}	QEHFQPTCSIKDRPA
AT4G09320	C_{43}	C_{2}	******MCGLYINLF
AT4G09320	C_{268}	-	-
AT4G11150	C_{201}	C_{121}	LKDLIVQCLLRLKEP
AT4G11150	-	C_{134}	EPSVLLRCREEDLGL

Table 5. Cont.

Accession number	Cys-NO site identified by BS-ICAT	Cys-NO site predicted by GPS-SNO	NO-peptide sequence predicted by GPS-SNO
AT4G11650	C_{72}	-	-
AT4G13430	C_{376}	C_{12}	ISSSPFLCKSSSKSD
AT4G13940	C_{244}	C_{42}	EMPGLMACRTEFGPS
AT4G13940	C_{268}	-	-
AT4G33030	C_{357}	$\mathbf{C}_{357}$	DIRDTVQCVEIAIAN
AT4G33030	-	C_{9}	AHLLSASCPSVISLS
AT5G02500	C_{319}	$\mathbf{C}_{319}$	NMDLFRKCMEPVEKC
AT5G02500	-	C_{326}	CMEPVEKCLRDAKMD
AT5G02500	-	C_{609}	MKELESICNPIIAKM
AT5G14040	C_{104}	C_{194}	IIADIALCPFEAVKV
AT5G15490	C_{350}	-	-
AT5G25100	C_{104}	C_{363}	YVGTGVQCLGMVLVT
AT5G44340	C_{354}	$\mathbf{C}_{354}$	NNVKSSVCDIAPKGL
AT5G44340	-	C_{12}	LHIQGGQCGNQIGAK
AT5G44340	-	C_{238}	ATMSGVTCCLRFPGQ
AT5G61790	C_{108}	-	-
AT5G62690	C_{56}	C_{12}	LHIQGGQCGNQIGAK
AT5G62690	C_{301}	C_{238}	ATMSGVTCCLRFPGQ
AT5G62690	-	C_{354}	NNVKSTVCDIPPTGL
AT5G66760	-	C_{4}	****MWRCVSRGFRA
AT5G66760	-	C_{77}	EHGFNTACITKLFPT
AT5G66760	-	C_{294}	TGIYGAGCLITEGSR
AT5G66760	-	C_{457}	IVVFGRACANRVAEI
AT5G66760	C_{526}	$\mathbf{C}_{526}$	QETLEEGCQLIDKAW
ATCG00340	C_{559}	-	-
ATCG00490	C_{192}	-	-
ATCG00490	C_{427}	-	-

S-nitrosylated *Arabidopsis* candidate proteins published by Fares *et al.* (2011) were analysed by GPS-SNO software using the medium threshold condition.
C in bold, matched cysteine residues.
doi:10.1371/journal.pone.0110232.t005

cysteine sites, the GPS-SNO program was used to predict 60 putative S-nitrosylation sites within these 34 proteins; however, only 11 of the predicted S-nitrosylation sites corresponded to sites identified using BS-ICAT (Table 6). These data indicate that the GPS-SNO software predicts a different set of S-nitrosylation sites in comparison to the BST-based approach.

Conclusions

Protein S-nitrosylation has emerged as an important field of the study of post-translational modification and is increasingly studied in plants. However, the proteomic approaches used to identify proteins that are targets of S-nitrosylation are associated with a variety of technical difficulties, such as the existence of side reactions in multi-step procedures, the low abundance or instability of proteins, and instrumental inaccuracy. Computational methods can help to overcome these problems. Computational analyses can be performed easily on complex protein datasets obtained from databases, regardless of protein abundance or instability or the existence of complex chemical reactions. However, computational approaches also present disadvantages. Protein S-nitrosylation is an enzyme-independent chemical

Table 6. Computational analysis of proteins, which *S*-nitrosylation sites were identified by BS-ICAT technology [28].

	BS-ICAT	GPS-SNO 1.0 medium threshold
Protein number	46	34
Total number of Cys-NO	53	60
Matched Cys-NO with BS-ICAT	-	11

doi:10.1371/journal.pone.0110232.t006

reaction that depends on many factors, all of which define whether a given cysteine residue will be sensitive to this modification. Although GPS-SNO 1.0 appears to predict S-nitrosylation sites with better accuracy, sensitivity, and specificity than other algorithms (Table S1), further research is required to improve the accuracy of the identification of S-nitrosylated sites. In this context, a set of non-SNO proteins would be helpful to calculate the sensitivity and specificity of the predictor.

Of greatest importance, all developed programs, including GPS-SNO 1.0, are based on the primary sequence of the studied proteins. However, the 3-dimensional (3D) structure of a protein also greatly affects its sensitivity to S-nitrosylation. The 3D structure defines which cysteine residues are accessible, and the amino acids surrounding a cysteine residue in the 3D structure determine the sensitivity of this residue to S-nitrosylation. Knowledge of the tertiary and quaternary structure of the protein may identify additional cysteines that might not be identified based on the primary sequence. Conversely, cysteine residues that are predicted to be S-nitrosylation targets might be excluded because they are inaccessible based on the spatial conformation. Therefore, knowledge of the high-resolution structure of the microenvironment around each cysteine residue is essential for defining the physicochemical features that determine S-nitrosylation specificity. Protein 3D structures have been already used to identify protein phosphorylation sites [84]. In that study linear motifs and spatial amino acid composition within a specific radial distance from the phosphorylated amino acid residue have been included [84]. But in general, computer-based prediction of S-nitrosylation candidates from *Arabidopsis* can offer a starting point for experimental verification and for further studies of S-nitrosylation in plants. The combination of computational prediction and experimental verification represents a good approach to better understand the molecular mechanisms and the regulatory functions of S-nitrosylation in plants. Nevertheless, both methods must be developed further to improve the precision with which S-nitrosylation targets are identified. Finally, the identified or predicted candidates must be confirmed using recombinant proteins, cysteine mutants and *in-vivo* approaches.

Supporting Information

Figure S1 Functional distribution of the 10% of candidates that were predicted with the highest confidence levels based on the MapMan Ontology of *Arabidopsis* proteins (http://mapman.gabipd.org/web/guest/mapman). Others: functional classes with less than 5% of S-nitrosylated candidates.
(TIF)

Table S1 Comparison of the performance of four software tools in predicting S-nitrosylation sites. Accuracy, sensitivity and specificity were used to evaluate the performance.
(DOCX)

Table S2 The *Arabidopsis* proteome was extracted from the TAIR 10 database, and proteins were assigned to cellular localizations according to the gene ontology cellular component classification.
(XLS)

Table S3 Amino acid sequences were downloaded for *Arabidopsis* from TAIR (www.arabidopsis.org) and analyzed using the GPS-SNO 1.0 program and the medium threshold. The 10% of candidates that were predicted with the highest confidence were ranked by the raw score divided by the cutoff of a particular cluster.
(XLSX)

Table S4 The *Arabidopsis* proteome was extracted from the TAIR 10 database, and proteins were assigned to cellular localizations according to the gene ontology cellular component classification.
(XLS)

Text S1 Subcellular compartments assigned according to the gene ontology cellular component classification (http://amigo1.geneontology.org/cgi-bin/amigo/go.cgi).
(DOC)

Author Contributions

Conceived and designed the experiments: MC IK MS CL. Performed the experiments: MC IK MS. Analyzed the data: MC IK MS CL. Contributed reagents/materials/analysis tools: MS. Wrote the paper: MC IK MS CL.

References

1. Durner J, Wendehenne D, Klessig DF (1998) Defense gene induction in tobacco by nitric oxide, cyclic GMP, and cyclic ADP-ribose. Proc Natl Acad Sci U S A 95: 10328–10333.
2. Delledonne M, Xia Y, Dixon RA, Lamb C (1998) Nitric oxide functions as a signal in plant disease resistance. Nature 394: 585–588.
3. Garcia-Mata C, Lamattina L (2002) Nitric oxide and abscisic acid cross talk in guard cells. Plant Physiol 128: 790–792.
4. Lombardo MC, Graziano M, Polacco JC, Lamattina L (2006) Nitric oxide functions as a positive regulator of root hair development. Plant Signal Behav 1: 28–33.
5. Corpas FJ, Chaki M, Fernandez-Ocana A, Valderrama R, Palma JM, et al. (2008) Metabolism of reactive nitrogen species in pea plants under abiotic stress conditions. Plant Cell Physiol 49: 1711–1722.
6. Chaki M, Fernandez-Ocana AM, Valderrama R, Carreras A, Esteban FJ, et al. (2009) Involvement of reactive nitrogen and oxygen species (RNS and ROS) in sunflower-mildew interaction. Plant Cell Physiol 50: 265–279.
7. Sirova J, Sedlarova M, Piterkova J, Luhova L, Petrivalsky M (2011) The role of nitric oxide in the germination of plant seeds and pollen. Plant Sci 181: 560–572.
8. Chaki M, Valderrama R, Fernandez-Ocana AM, Carreras A, Gomez-Rodriguez MV, et al. (2011) Mechanical wounding induces a nitrosative stress by down-regulation of GSNO reductase and an increase in S-nitrosothiols in sunflower (Helianthus annuus) seedlings. J Exp Bot 62: 1803–1813.
9. Begara-Morales JC, Chaki M, Sanchez-Calvo B, Mata-Perez C, Leterrier M, et al. (2013) Protein tyrosine nitration in pea roots during development and senescence. J Exp Bot 64: 1121–1134.
10. Hess DT, Matsumoto A, Kim SO, Marshall HE, Stamler JS (2005) Protein S-nitrosylation: purview and parameters. Nat Rev Mol Cell Biol 6: 150–166.
11. Cho DH, Nakamura T, Fang J, Cieplak P, Godzik A, et al. (2009) S-nitrosylation of Drp1 mediates beta-amyloid-related mitochondrial fission and neuronal injury. Science 324: 102–105.
12. Guo CJ, Atochina-Vasserman EN, Abramova E, Foley JP, Zaman A, et al. (2008) S-nitrosylation of surfactant protein-D controls inflammatory function. PLoS Biol 6: e266.
13. Hao G, Xie L, Gross SS (2004) Argininosuccinate synthetase is reversibly inactivated by S-nitrosylation in vitro and in vivo. J Biol Chem 279: 36192–36200.
14. Jaffrey SR, Snyder SH (2001) The biotin switch method for the detection of S-nitrosylated proteins. Sci STKE 2001: pl1.
15. Hao G, Derakhshan B, Shi L, Campagne F, Gross SS (2006) SNOSID, a proteomic method for identification of cysteine S-nitrosylation sites in complex protein mixtures. Proc Natl Acad Sci U S A 103: 1012–1017.
16. Lindermayr C, Saalbach G, Durner J (2005) Proteomic identification of S-nitrosylated proteins in *Arabidopsis*. Plant Physiol 137: 921–930.
17. Abat JK, Mattoo AK, Deswal R (2008) S-nitrosylated proteins of a medicinal CAM plant Kalanchoe pinnata- ribulose-1,5-bisphosphate carboxylase/oxygenase activity targeted for inhibition. FEBS J 275: 2862–2872.
18. Palmieri MC, Lindermayr C, Bauwe H, Steinhauser C, Durner J (2010) Regulation of plant glycine decarboxylase by s-nitrosylation and glutathionylation. Plant Physiol 152: 1514–1528.

19. Lindermayr C, Sell S, Muller B, Leister D, Durner J (2010) Redox regulation of the NPR1-TGA1 system of Arabidopsis thaliana by nitric oxide. Plant Cell 22: 2894–2907.
20. Begara-Morales JC, Sanchez-Calvo B, Chaki M, Valderrama R, Mata-Perez C, et al. (2013) Dual regulation of cytosolic ascorbate peroxidase (APX) by tyrosine nitration and S-nitrosylation. J Exp Bot.
21. Spadaro D, Yun BW, Spoel SH, Chu C, Wang YQ, et al. (2010) The redox switch: dynamic regulation of protein function by cysteine modifications. Physiol Plant 138: 360–371.
22. Stamler JS, Lamas S, Fang FC (2001) Nitrosylation. the prototypic redox-based signaling mechanism. Cell 106: 675–683.
23. Taldone FS, Tummala M, Goldstein EJ, Ryzhov V, Ravi K, et al. (2005) Studying the S-nitrosylation of model peptides and eNOS protein by mass spectrometry. Nitric Oxide 13: 176–187.
24. Greco TM, Hodara R, Parastatidis I, Heijnen HF, Dennehy MK, et al. (2006) Identification of S-nitrosylation motifs by site-specific mapping of the S-nitrosocysteine proteome in human vascular smooth muscle cells. Proc Natl Acad Sci U S A 103: 7420–7425.
25. Marino SM, Gladyshev VN (2010) Structural analysis of cysteine S-nitrosylation: a modified acid-based motif and the emerging role of trans-nitrosylation. J Mol Biol 395: 844–859.
26. Kovacs I, Lindermayr C (2013) Nitric oxide-based protein modification: formation and site-specificity of protein S-nitrosylation. Front Plant Sci 4: 137.
27. Romero-Puertas MC, Campostrini N, Matte A, Righetti PG, Perazzolli M, et al. (2008) Proteomic analysis of S-nitrosylated proteins in Arabidopsis thaliana undergoing hypersensitive response. Proteomics 8: 1459–1469.
28. Fares A, Rossignol M, Peltier JB (2011) Proteomics investigation of endogenous S-nitrosylation in Arabidopsis. Biochem Biophys Res Commun 416: 331–336.
29. Tanou G, Job C, Rajjou L, Arc E, Belghazi M, et al. (2009) Proteomics reveals the overlapping roles of hydrogen peroxide and nitric oxide in the acclimation of citrus plants to salinity. Plant J 60: 795–804.
30. Lin A, Wang Y, Tang J, Xue P, Li C, et al. (2012) Nitric oxide and protein S-nitrosylation are integral to hydrogen peroxide-induced leaf cell death in rice. Plant Physiol 158: 451–464.
31. Ortega-Galisteo AP, Rodriguez-Serrano M, Pazmino DM, Gupta DK, Sandalio LM, et al. (2012) S-Nitrosylated proteins in pea (Pisum sativum L.) leaf peroxisomes: changes under abiotic stress. J Exp Bot 63: 2089–2103.
32. Astier J, Besson-Bard A, Lamotte O, Bertoldo J, Bourque S, et al. (2012) Nitric oxide inhibits the ATPase activity of the chaperone-like AAA+ ATPase CDC48, a target for S-nitrosylation in cryptogein signalling in tobacco cells. Biochem J 447: 249–260.
33. Astier J, Kulik A, Koen E, Besson-Bard A, Bourque S, et al. (2012) Protein S-nitrosylation: what's going on in plants? Free Radic Biol Med 53: 1101–1110.
34. Xue Y, Liu Z, Cao J, Ren J (2011) Computational Prediction of Post-Translational Modification Sites in Proteins. book edited by Ning-Sun Yang: 105–124.
35. Song C, Ye M, Liu Z, Cheng H, Jiang X, et al. (2012) Systematic analysis of protein phosphorylation networks from phosphoproteomic data. Mol Cell Proteomics 11: 1070–1083.
36. Ren J, Wen L, Gao X, Jin C, Xue Y, et al. (2008) CSS-Palm 2.0: an updated software for palmitoylation sites prediction. Protein Eng Des Sel 21: 639–644.
37. Ren J, Gao X, Jin C, Zhu M, Wang X, et al. (2009) Systematic study of protein sumoylation: Development of a site-specific predictor of SUMOsp 2.0. Proteomics 9: 3409–3412.
38. Liu Z, Cao J, Ma Q, Gao X, Ren J, et al. (2011) GPS-YNO2: computational prediction of tyrosine nitration sites in proteins. Mol Biosyst 7: 1197–1204.
39. Lee TY, Chen YJ, Lu TC, Huang HD, Chen YJ (2011) SNOSite: exploiting maximal dependence decomposition to identify cysteine S-nitrosylation with substrate site specificity. PLoS One 6: e21849.
40. Xu Y, Ding J, Wu LY, Chou KC (2013) iSNO-PseAAC: predict cysteine S-nitrosylation sites in proteins by incorporating position specific amino acid propensity into pseudo amino acid composition. PLoS One 8: e55844.
41. Xu Y, Shao XJ, Wu LY, Deng NY, Chou KC (2013) iSNO-AAPair: incorporating amino acid pairwise coupling into PseAAC for predicting cysteine S-nitrosylation sites in proteins. PeerJ 1: e171.
42. Xue Y, Liu Z, Gao X, Jin C, Wen L, et al. (2010) GPS-SNO: computational prediction of protein S-nitrosylation sites with a modified GPS algorithm. PLoS One 5: e11290.
43. Sun J, Morgan M, Shen RF, Steenbergen C, Murphy E (2007) Preconditioning results in S-nitrosylation of proteins involved in regulation of mitochondrial energetics and calcium transport. Circ Res 101: 1155–1163.
44. Doulias PT, Greene JL, Greco TM, Tenopoulou M, Seeholzer SH, et al. (2010) Structural profiling of endogenous S-nitrosocysteine residues reveals unique features that accommodate diverse mechanisms for protein S-nitrosylation. Proc Natl Acad Sci U S A 107: 16958–16963.
45. Kato H, Takemoto D, Kawakita K (2013) Proteomic analysis of S-nitrosylated proteins in potato plant. Physiol Plant 148: 371–386.
46. Frohlich A, Gaupels F, Sarioglu H, Holzmeister C, Spannagl M, et al. (2012) Looking deep inside: detection of low-abundance proteins in leaf extracts of Arabidopsis and phloem exudates of pumpkin. Plant Physiol 159: 902–914.
47. Xue Y, Ren J, Gao X, Jin C, Wen L, et al. (2008) GPS 2.0, a tool to predict kinase-specific phosphorylation sites in hierarchy. Mol Cell Proteomics 7: 1598–1608.
48. Schippers JH, Nguyen HM, Lu D, Schmidt R, Mueller-Roeber B (2012) ROS homeostasis during development: an evolutionary conserved strategy. Cell Mol Life Sci 69: 3245–3257.
49. Holzmeister C, Frohlich A, Sarioglu H, Bauer N, Durner J, et al. (2011) Proteomic analysis of defense response of wildtype Arabidopsis thaliana and plants with impaired NO- homeostasis. Proteomics 11: 1664–1683.
50. Kwon E, Feechan A, Yun BW, Hwang BH, Pallas JA, et al. (2012) AtGSNOR1 function is required for multiple developmental programs in Arabidopsis. Planta 236: 887–900.
51. Kohr MJ, Evangelista AM, Ferlito M, Steenbergen C, Murphy E (2014) S-nitrosylation of TRIM72 at cysteine 144 is critical for protection against oxidation-induced protein degradation and cell death. J Mol Cell Cardiol 69: 67–74.
52. Chen YY, Chu HM, Pan KT, Teng CH, Wang DL, et al. (2008) Cysteine S-nitrosylation protects protein-tyrosine phosphatase 1B against oxidation-induced permanent inactivation. J Biol Chem 283: 35265–35272.
53. Christian JO, Braginets R, Schulze WX, Walther D (2012) Characterization and Prediction of Protein Phosphorylation Hotspots in Arabidopsis thaliana. Front Plant Sci 3: 207.
54. Ng JY, Boelen L, Wong JW (2013) Bioinformatics analysis reveals biophysical and evolutionary insights into the 3-nitrotyrosine post-translational modification in the human proteome. Open Biol 3: 120148.
55. Chen YJ, Ku WC, Lin PY, Chou HC, Khoo KH, et al. (2010) S-alkylating labeling strategy for site-specific identification of the s-nitrosoproteome. J Proteome Res 9: 6417–6439.
56. Baier M, Dietz KJ (2005) Chloroplasts as source and target of cellular redox regulation: a discussion on chloroplast redox signals in the context of plant physiology. Journal of Experimental Botany 56: 1449–1462.
57. Allen JF, Santabarbara S, Allen CA, Puthiyaveetil S (2011) Discrete Redox Signaling Pathways Regulate Photosynthetic Light-Harvesting and Chloroplast Gene Transcription. Plos One 6.
58. Galatro A, Puntarulo S, Guiamet JJ, Simontacchi M (2013) Chloroplast functionality has a positive effect on nitric oxide level in soybean cotyledons. Plant Physiology and Biochemistry 66: 26–33.
59. Tewari RK, Prommer J, Watanabe M (2013) Endogenous nitric oxide generation in protoplast chloroplasts. Plant cell reports 32: 31–44.
60. Misra AN, Vladkova R, Singh R, Misra M, Dobrikova AG, et al. (2014) Action and target sites of nitric oxide in chloroplasts. Nitric Oxide-Biology and Chemistry 39: 35–45.
61. Abat JK, Deswal R (2009) Differential modulation of S-nitrosoproteome of *Brassica juncea* by low temperature: change in S-nitrosylation of Rubisco is responsible for the inactivation of its carboxylase activity. Proteomics 9: 4368–4380.
62. Tanou G, Filippou P, Belghazi M, Job D, Diamantidis G, et al. (2012) Oxidative and nitrosative-based signaling and associated post-translational modifications orchestrate the acclimation of citrus plants to salinity stress. Plant J 72: 585–599.
63. Zaffagnini M, Michelet L, Sciabolini C, Di Giacinto N, Morisse S, et al. (2014) High-resolution crystal structure and redox properties of chloroplastic triosephosphate isomerase from Chlamydomonas reinhardtii. Mol Plant 7: 101–120.
64. Tzafrir I, Pena-Muralla R, Dickerman A, Berg M, Rogers R, et al. (2004) Identification of genes required for embryo development in Arabidopsis. Plant Physiology 135: 1206–1220.
65. Pinon V, Etchells JP, Rossignol P, Collier SA, Arroyo JM, et al. (2008) Three PIGGYBACK genes that specifically influence leaf patterning encode ribosomal proteins. Development 135: 1315–1324.
66. Yao Y, Ling QH, Wang H, Huang H (2008) Ribosomal proteins promote leaf adaxial identity. Development 135: 1325–1334.
67. Fujikura U, Horiguchi G, Ponce MR, Micol JL, Tsukaya H (2009) Coordination of cell proliferation and cell expansion mediated by ribosome-related processes in the leaves of Arabidopsis thaliana. Plant Journal 59: 499–508.
68. Ferreyra MLF, Pezza A, Biarc J, Burlingame AL, Casati P (2010) Plant L10 Ribosomal Proteins Have Different Roles during Development and Translation under Ultraviolet-B Stress. Plant Physiology 153: 1878–1894.
69. Rosado A, Sohn EJ, Drakakaki G, Pan SQ, Swidergal A, et al. (2010) Auxin-Mediated Ribosomal Biogenesis Regulates Vacuolar Trafficking in Arabidopsis. Plant Cell 22: 143–158.
70. Szakonyi D, Byrne ME (2011) Ribosomal protein L27a is required for growth and patterning in Arabidopsis thaliana. Plant Journal 65: 269–281.
71. Pawloski JR, Hess DT, Stamler JS (2001) Export by red blood cells of nitric oxide bioactivity. Nature 409: 622–626.
72. Mannick JB, Schonhoff C, Papeta N, Ghafourifar P, Szibor M, et al. (2001) S-Nitrosylation of mitochondrial caspases. J Cell Biol 154: 1111–1116.
73. Camejo D, Romero-Puertas Mdel C, Rodriguez-Serrano M, Sandalio LM, Lazaro JJ, et al. (2013) Salinity-induced changes in S-nitrosylation of pea mitochondrial proteins. J Proteomics 79: 87–99.
74. Ckless K, Reynaert NL, Taatjes DJ, Lounsbury KM, van der Vliet A, et al. (2004) In situ detection and visualization of S-nitrosylated proteins following chemical derivatization: identification of Ran GTPase as a target for S-nitrosylation. Nitric Oxide 11: 216–227.
75. Zaman K, Carraro S, Doherty J, Henderson EM, Lendermon E, et al. (2006) S-nitrosylating agents: a novel class of compounds that increase cystic fibrosis transmembrane conductance regulator expression and maturation in epithelial cells. Mol Pharmacol 70: 1435–1442.

76. Sehrawat A, Deswal R (2014) S-Nitrosylation Analysis in Brassica juncea Apoplast Highlights the Importance of Nitric Oxide in Cold-Stress Signaling. J Proteome Res.
77. Liu M, Hou J, Huang L, Huang X, Heibeck TH, et al. (2010) Site-specific proteomics approach for study protein S-nitrosylation. Anal Chem 82: 7160–7168.
78. Kuncewicz T, Sheta EA, Goldknopf IL, Kone BC (2003) Proteomic analysis of s-nitrosylated proteins in mesangial cells. Mol Cell Proteomics 2: 156–163.
79. Ferl RJ, Manak MS, Reyes MF (2002) The 14-3-3s. Genome Biol 3: REVIEWS3010.
80. Maldonado-Alconada AM, Echevarría-Zomeño S, Lindermayr C, Redondo-López I, Durner J, et al. (2011) Proteomic analysis of Arabidopsis protein S-nitrosylation in response to inoculation with Pseudomonas syringae. Acta Physiol Plant 33: 1493–1514.
81. Belenghi B, Romero-Puertas MC, Vercammen D, Brackenier A, Inze D, et al. (2007) Metacaspase activity of *Arabidopsis thaliana* is regulated by S-nitrosylation of a critical cysteine residue. J Biol Chem 282: 1352–1358.
82. Perazzolli M, Dominici P, Romero-Puertas MC, Zago E, Zeier J, et al. (2004) *Arabidopsis* nonsymbiotic hemoglobin AHb1 modulates nitric oxide bioactivity. Plant Cell 16: 2785–2794.
83. Tada Y, Spoel SH, Pajerowska-Mukhtar K, Mou Z, Song J, et al. (2008) Plant immunity requires conformational changes [corrected] of NPR1 via S-nitrosylation and thioredoxins. Science 321: 952–956.
84. Su MG, Lee TY (2013) Incorporating substrate sequence motifs and spatial amino acid composition to identify kinase-specific phosphorylation sites on protein three-dimensional structures. BMC Bioinformatics 14 Suppl 16: S2.
85. Lindermayr C, Saalbach G, Bahnweg G, Durner J (2006) Differential inhibition of *Arabidopsis* methionine adenosyltransferases by protein S-nitrosylation. J Biol Chem 281: 4285–4291.
86. Romero-Puertas MC, Laxa M, Matte A, Zaninotto F, Finkemeier I, et al. (2007) S-nitrosylation of peroxiredoxin II E promotes peroxynitrite-mediated tyrosine nitration. Plant Cell 19: 4120–4130.
87. Holtgrefe S, Gohlke J, Starmann J, Druce S, Klocke S, et al. (2008) Regulation of plant cytosolic glyceraldehyde 3-phosphate dehydrogenase isoforms by thiol modifications. Physiol Plant 133: 211–228.
88. Wang YQ, Feechan A, Yun BW, Shafiei R, Hofmann A, et al. (2009) S-nitrosylation of AtSABP3 antagonizes the expression of plant immunity. J Biol Chem 284: 2131–2137.
89. Yun BW, Feechan A, Yin M, Saidi NB, Le Bihan T, et al. (2011) S-nitrosylation of NADPH oxidase regulates cell death in plant immunity. Nature 478: 264–268.
90. van der Linde K, Gutsche N, Leffers HM, Lindermayr C, Muller B, et al. (2011) Regulation of plant cytosolic aldolase functions by redox-modifications. Plant Physiol Biochem 49: 946–957.
91. Terrile MC, Paris R, Calderon-Villalobos LI, Iglesias MJ, Lamattina L, et al. (2012) Nitric oxide influences auxin signaling through S-nitrosylation of the Arabidopsis TRANSPORT INHIBITOR RESPONSE 1 auxin receptor. Plant J 70: 492–500.
92. Tavares CP, Vernal J, Delena RA, Lamattina L, Cassia R, et al. (2014) S-nitrosylation influences the structure and DNA binding activity of AtMYB30 transcription factor from Arabidopsis thaliana. Biochim Biophys Acta 1844: 810–817.